

## DEVELOPMENT OF TREATMENT PLANNING SOFTWARE FOR CARBON-ION SCANNING AT HIMAC

T. Inaniwa, T. Furukawa, S. Sato, S. Mori, N. Kanematsu, K. Noda,  
National Institute of Radiological Sciences, Chiba, JAPAN  
T. Kanai, Gunma University, Maebashi, JAPAN

### *Abstract*

In order to use an intensity-controlled raster scan method at the new treatment facility in HIMAC, we have developed a code system dedicated to the planning of radiotherapy with the scanned  $^{12}\text{C}$  beam. Inverse planning techniques are implemented in the software in order to obtain the uniform biological dose distribution within the planned target volume (PTV) as well as reduce the dose delivered to the organ at risks (OARs) delineated on clinical CT images. The scan trajectory is determined so that the path length will be minimized by applying a fast simulated annealing algorithm for scan trajectory optimisation. Furthermore, the extra dose inevitably delivered to the irradiated site during the beam transition time from one spot to the next spot is integrated into the inverse planning process to shorten the treatment time. The code also copes with the planning for intensity modulated ion therapy (IMIT). The reliability of the developed code has been confirmed through the irradiation experiments at the secondary beam line in HIMAC.

### INTRODUCTION

A project to construct a new treatment facility as an extension of the existing Heavy-Ion Medical Accelerator in Chiba (HIMAC) facility has been initiated for further development of carbon-ion therapy at the National Institute of Radiological Sciences (NIRS). The new treatment facility will be equipped with three treatment rooms, two of them will provide the horizontal and vertical fixed beam ports, and another one a rotating gantry [1]. In all rooms, three-dimensional (3D) irradiation with pencil beam scanning will be utilized in order to make full use of the advantages of heavy-ion therapy such as high dose concentration and high relative biological effectiveness (RBE) around the Bragg peak. This method has already been implemented for clinical use at the Paul Scherrer Institute (PSI) with protons [2] and the Gesellschaft für Schwerionenforschung mbH (GSI) with carbon ions [3]. In the new facility, we intend to treat not only static tumors but also moving tumors by using gated irradiation and re-scanning methods. In order to complete the treatment irradiation within a few minutes with these methods, the fast scanning is the key in the development [4]. For this purpose, we developed an inverse planning code dedicated to radiotherapy with the scanned  $^{12}\text{C}$  beam which suits for the unique scanning system designed at the new treatment facility in HIMAC. This paper describes the basic principles of the code.

### METHODS AND MATERIALS

#### *Beam Model*

In 3D irradiation with pencil beam scanning, the prescribed dose distribution can be achieved by superimposing the dose of the individual pencil beams  $d$  with different stopping positions according to the optimized weights  $w$  for these beams. The Bragg peak of the pristine beam is slightly broadened to produce a “mini peak” by the ridge filter, and is used as a pencil beam. In the new treatment facility, pristine beams with about 10 individual energies will be prepared between 140 MeV/u to 430 MeV/u. The dose response at a point  $(x_i, y_i, z_i)$  delivered by the pencil beam stopped at  $(x_0, y_0, z_0)$  can be represented as follows:

$$d(x_i, y_i, z_i; x_0, y_0, z_0) = d_x(x_i; x_0, \sigma_x(z_i; z_0)) d_y(y_i; y_0, \sigma_y(z_i; z_0)) d_z(z_i; z_0) \quad (1)$$

Here,  $d_z(z_i; z_0)$  is the integrated dose at a depth of  $z_i$ . On the other hand,  $d_x(x_i; x_0, \sigma_x(z_i; z_0))$  and  $d_y(y_i; y_0, \sigma_y(z_i; z_0))$  are the normalized Gaussian functions with standard deviations  $\sigma_x(z_i; z_0)$  and  $\sigma_y(z_i; z_0)$  representing the beam spread at a depth  $z_i$ . The integrated dose  $d_z(z_i; z_0)$  and the lateral beam spread, i.e.,  $\sigma_x(z_i; z_0)$  and  $\sigma_y(z_i; z_0)$ , were determined from the measured dose distribution with a large area parallel plate ionisation chamber and the profile monitor, respectively. Then they are fitted to simple formulae and incorporated into the planning software. With this algorithm, the effect of the beam spread due to multiple scattering in range shifter can be incorporated, at least for the primary particles. However, our recent research revealed that the field-size effect of the dose will occur also in carbon ion scanning with range shifter plates [5]. In order to account for this effect, the novel pencil beam model, in which the lateral dose distribution is represented by a superposition of three Gaussians, was incorporated into the software. The beam model can optionally be used in optimization and/or recalculation process to determine the “predicted dose scaling factor” [5].

#### *Clinical Dose Calculation*

For scanning irradiation method, we employed the same biophysical model based on the linear quadratic (LQ) model as that for the passive irradiation [6] and the layer-stacking methods [7]. When a biological system is irradiated with scanned pencil beams within a sufficiently

short period of time, the survival at point  $(x_i, y_i, z_i)$  is derived by

$$S_{mix,i} = \exp\left[-\alpha_{mix,i} D_{phys,i} - \beta_{mix,i} D_{phys,i}^2\right] \quad (2)$$

In the above equation,  $D_{phys,i}$  is the physical dose at the point  $i$  delivered by the scanned pencil beams with their weights  $w$ .  $\alpha_{mix}$  and  $\beta_{mix}$  are the dose averaged values of coefficients  $\alpha$  and  $\beta$  in the LQ model at  $(x_i, y_i, z_i)$  [6]. The biological RBE at  $(x_i, y_i, z_i)$  can be obtained from the ratio between the doses required to obtain a desired level of cell killing, i.e. survival level  $S$ , by a reference radiation quality (Co-60) and by the carbon beam. The survival level of 10% for HSG cells is used in the biological RBE calculation independent of the dose levels. Then, the clinical RBE are derived by multiplying the clinical factor 1.43 to the biological RBE in order to account for the difference between *in vivo* and *in vitro*. Finally, the clinical dose in units of GyE at the point,  $D_{biol,i}$ , can be calculated by

$$D_{biol,i} = D_{phys,i} \times RBE_i(S) \quad (3)$$

### Dose Optimization

The goal of dose optimisation in treatment planning software is to find the best particle numbers (weight) and positions of all rasterpoints, i.e. the best weighting matrix, so that the resulting dose distribution is as close as possible to the prescribed dose distribution within the target volume and does not exceed the dose restrictions within the OARs. In determination of the weighting matrix, the dose-based objective function  $f(w)$  is minimized through an iterative optimisation process. The objective function can be described as;

$$f(w) = \sum_{i \in T} \left[ Q_p^o [D_{biol,i}(w) + U_i - D_p^{\max}]_+^2 + Q_p^u [D_p^{\min} + U_i - D_{biol,i}(w)]_+^2 \right] + \sum_{i \in O} Q_o [D_{biol,i}(w) + U_i - D_o^{\max}]_+^2 \quad (4)$$

where  $D_{biol,i}(w)$ ,  $D_p^{\max}$ ,  $D_p^{\min}$ ,  $Q_p^o$ ,  $Q_p^u$ ,  $D_o^{\max}$ ,  $Q_o$  are the biological dose at a point  $i$  obtained with matrix  $w$ , the maximum and minimum doses applied to the target  $T$ , the penalties for over- and underdosage specified for the target, the maximum dose allowed for the OAR and the penalty for overdosage in OAR, respectively. In raster scanning irradiation, the beam delivery is not switched off during the transition time from one spot to the next. Therefore, in this scheme, the extra dose is inevitably delivered to the sites between two successive spots during the beam spot transition, along the scan trajectory. The contribution of extra dose is included in the optimization process by adding the term  $U_i$  to the objective function representing the amount of the extra dose delivered to a voxel  $i$  [8]. The objective function (4) is minimized by applying the iterative minimization algorithm based on

quasi-Newton method, and the best weighting matrix  $w$  can be obtained for each rasterpoint.

### Flow of Treatment Planning

By using the developed software, the treatment plans are produced according to the following steps. (a) Radio-oncologists delineate the PTV and OARs on the clinical CT images using an external platform, and determine the primary treatment parameters, e.g. isocenter, desired dose level, number of ports, and beam directions. Then, these data are imported to the developed software. (b) The CT images are stored into the dose calculation region by using the tri-linear interpolation. The voxels within the PTV and OARs are identified with different flags within the dose calculation region. (c) The x-ray CT numbers stored into each voxel is converted to the effective density for therapeutic carbon beam based on the polybinary tissue model [9]. (d) The position of all rasterpoints are determined automatically from the PTV so as to account for the dose fall-off at the longitudinal and lateral edges of the PTV due to the finite size of the mini peak and beam width. (e) From the information about the maximum range found in (d), the optimum beam energy is selected among 10 individual energies prepared in the HIMAC synchrotron. (f) In order to minimize the extra dose in raster scanning and shorten the treatment time, we determined the scan trajectory on each slice so that the path length would be minimized by applying a fast simulated annealing algorithm to scan trajectory optimization. (g) The particle numbers (weight) for each raster-point are determined by the dose optimization method described in the previous section. (h) Finally, the beam steering file is produced in which the position of the raster-point  $x_0, y_0, z_0$ , corresponding thickness of the range shifter plates, and the particle numbers (weights) of all pencil beams are written in following the order of the optimized scan trajectory.

## RESULTS AND DISCUSSIONS

In order to investigate the clinical applicability of the developed software, treatment plans are produced for data of patients treated at HIMAC. We can produce both a single field plan and an IMIT plan with the software.

### Single Field Planning

As an example of single field planning, a patient having bone and soft tissue sarcoma was selected (Fig. 1). The biological dose of 1.0 GyE is delivered from a single port in the anterior to posterior direction. In this plan, only the target volume is specified on the CT images and implemented for dose optimization. The maximum and minimum doses applied to the PTV is 1.0 GyE and the penalties for over- and underdosage are 6 and 8, respectively. The voxel resolution as well as the scanner step sizes,  $\Delta x$  and  $\Delta y$ , and step size of range shifter plate,  $\Delta z$ , were set to 2.0 mm. The beam energy determined for the plan was 350 MeV/u, and the total of 36351 rasterpoints was located within the rasterpoint

region. In Fig. 1 the planned distributions of the biological dose are shown with color-wash display on axial, sagittal and frontal CT images. We can see that highly conformal biological dose distribution can be achieved within the PTV.

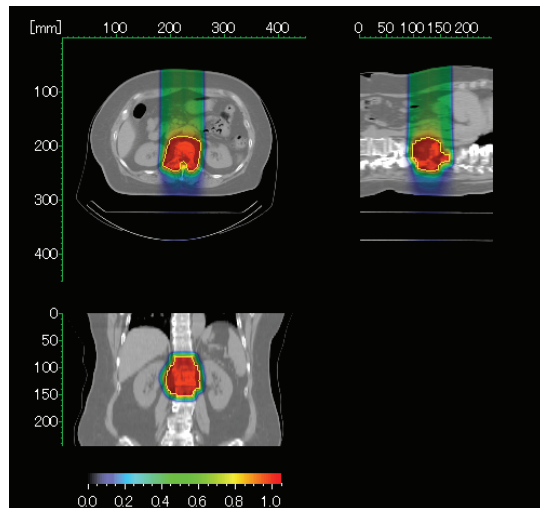


Figure 1: CT images with color-wash display of biological dose distribution. The PTV is identified with yellow curve on each CT image.

In order to verify the developed software, we carried out irradiation experiments at the secondary beam line (SBL) in HIMAC. In the experiments, a carbon pencil beam with an intensity of  $6.0 \times 10^6$  particles/s was scanned in a water vessel according to the beam steering file obtained for the plan shown in Fig. 1. The physical dose distributions are measured with a beam profile monitor by moving it stepwise along the beam axis in a water vessel. In Fig. 2, the physical dose distributions measured with the monitor (open circles) are compared with the recalculated ones in water according to the derived beam steering file (red curves). Good agreement between them implies that the prescribed biological dose distribution (black curve) is also realized at the PTV.

### IMIT Planning

As an example of the intensity modulated ion therapy (IMIT) planning, an RTOG benchmark phantom was selected (see Fig. 3(a)). A five equidistant, coplanar beam setup was chosen for the treatment plan. Two types of plans were generated, a plan that considers each of the five fields separately and an IMIT plan, in order to investigate the effectiveness of an IMIT. For both plans, the maximum and minimum doses to the target and the maximum dose to the OAR were 5.1, 4.9 and 2.0 GyE, respectively. In Fig. 3(b), the clinical dose distribution by a IMIT plan is shown with color-wash display. It can be seen that the OAR could be spared in each beam port. The mean dose delivered to the OAR could be reduced by a factor of three using the IMIT plan without any large deterioration in dose conformation to the PTV as compared to the single-field plan.

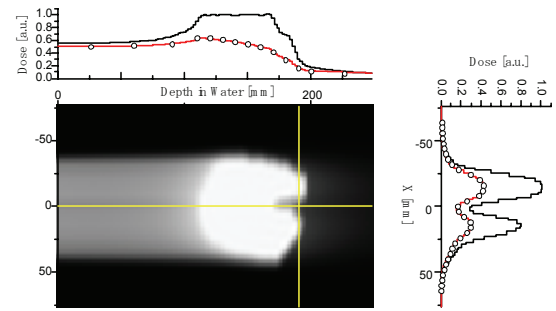


Figure 2: The physical dose distribution measured with the beam profile monitor (open circles) and the recalculated one (red curve) on the x-z plane at  $y=0$  mm. In the figure, the black curve indicates the expected biological dose distribution.

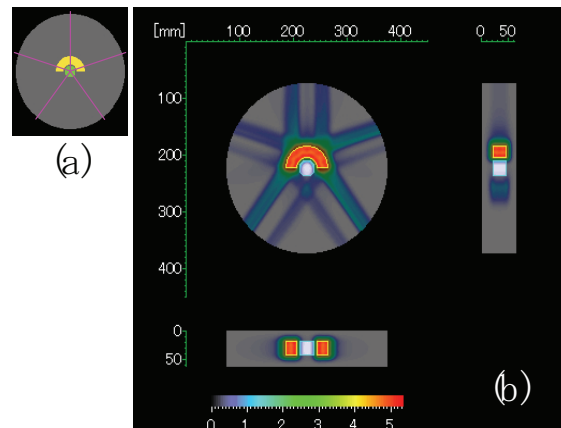


Figure 3: (a) RTOG benchmark phantom. Target and OAR are specified with yellow and green colours, respectively. (b) The color-wash display of clinical dose distribution planned with a five equidistant, coplanar beam setup using IMIT procedure.

## SUMMARY

We have developed the inverse planning software for an intensity-controlled raster scan method with carbon ions, which is to be used at the new treatment facility in HIMAC. The reliability of the software was confirmed through the irradiation experiments at the SBL in HIMAC.

## REFERENCES

- [1] K. Noda et al., J Radiat Res. 48 (2007) Suppl. A43.
- [2] E. Pedroni et al., Med Phys. 22 (1995) 37.
- [3] G. Kraft, Nucl Instr Meth. A 454 (2000) 1.
- [4] T. Furukawa, Med Phys. 34 (2007) 1085.
- [5] T. Inaniwa et al., Med Phys. (in press).
- [6] T. Kanai et al., Int J Rad Onc Bio Phys. 44 (1999) 201.
- [7] N. Kanematsu et al., Med Phys. 29 (2002) 2823.
- [8] T. Inaniwa et al., Med Phys. 34 (2007) 3302.
- [9] N. Kanematsu et al., Phys Med Biol. 48 (2003) 1053.